η6-Coordinated ruthenabenzenes from three-component assembly on a diruthenium μ-allenyl scaffold

η^6-Coordinated Ruthenabenzenes fromThree-Component Assembly on a Diruthenium μ-Allenyl Scaffold

Giulio Bresciani,[a,d] Stefano Zacchini,[b,d] Guido Pampaloni,[a,d] Marco Bortoluzzi,[c,d] Fabio Marchetti,[a,d,*]

[a] University of Pisa, Department of Chemistry and Industrial Chemistry, Via G. Moruzzi 13, I-56124 Pisa, Italy.

[b] University of Bologna, Department of Industrial Chemistry "Toso Montanari", Viale Risorgimento 4, I-40136 Bologna, Italy.

[c] University of Venezia "Ca' Foscari", Department of Molecular Science and Nanosystems, Via Torino 155, I-30170 Mestre (VE), Italy.

[d] CIRCC, Via Celso Ulpiani 27, I-70126 Bari, Italy.

Corresponding Author

*E-mail address: fabio.marchetti1974@unipi.it

Abstract

The room temperature reactions with internal alkynes,RC≡CR,of the μ-allenyl acetonitrile complex $[Ru_2Cp_2(CO)_2(NCMe)\{\mu\text{-}\eta^1\text{:}\eta^2\text{-}C^1H\text{=}C^2\text{=}C^3Me_2\}]BF_4$ (**1-NCMe**), freshly prepared from the tricarbonyl precursor $[Ru_2Cp_2(CO)_3\{\mu\text{-}\eta^1\text{:}\eta^2\text{-}C^1H\text{=}C^2\text{=}C^3Me_2\}]BF_4$, **1**, proceeded with alkyne insertion into ruthenium-allenyl bond and allenyl-CO coupling, affording compounds $[Ru_2Cp_2(CO)_2\{\mu\text{-}\eta^2\text{:}\eta^5\text{-}C(R)C(R)C^1HC^2(C^3Me{=}CH_2)C(OH)\}]BF_4$ (R = Ph, **2**; R = CO_2Me, **3**; R = CO_2Et, **4**) in 83-94% yields. Deprotonation of **2-4** by triethylamine gave $[Ru_2Cp_2(CO)_2\{\mu\text{-}\eta^2\text{:}\eta^5\text{-}C(R)C(R)CHC(CMe{=}CH_2)C(O)\}]$ (R = Ph, **5**; R = CO_2Me, **6**; R = CO_2Et, **7**) in 75-88% yields, and **2-4**could be recoveredupon $HBF_4{\cdot}Et_2O$ addition to **5-7**. All the products, **2-7**, were fully characterized by elemental analysis, IR and multinuclear NMR spectroscopy. The structure of **2** was ascertained by single crystal X-ray diffraction and investigated by DFT calculations, revealing a six-membered ruthenacyclewith Shannon aromaticity index in line with relatedcompounds. The formation of ruthenium-coordinated ruthenabenzenes from a preexistent diruthenium scaffold is a versatilebut underdeveloped approach exploiting cooperative effects typical of a dimetallic core.

Keywords: ruthenabenzene; diruthenium complexes; allenyl ligand; alkyne insertion; three-component reaction.

Introduction

The concept of metallabenzene (in general, an arene with a CH group formally replaced by a transition metal fragment) was introduced in 1979,[1] although the synthesis of the first representant of this family of organometallic compounds dates back to 1976, obtained from the reaction of $[RuH_2(CO)(PPh_3)_3]$ with methyl propiolate.[2] Then, this field of chemistry underwenta rapid development, stimulated by the fundamental interest with respect to the possible aromatic character of the metallacyclic structure and

the subsequent reactivity.[3,4,5]Thus, a wide variety of stable metallabenzenes has been synthesized and characterized, and the exploration of novel synthetic routes is still arousing considerable attention.[6]Ruthenabenzenes, which have recently witnessed a renewed interest due to their possible application as metathesis catalysts,[7] are usually accessible from monoruthenium precursors by means of different strategies.[6,8,9,10] However, *sandwich* compounds consisting of a ruthenabenzene acting as a η^6 organometallic ligand towards a second metal centre are significantly rarer and have been prepared mainly via ring closure reaction of open pentadienyl ligands with a suitable metal fragment (Scheme 1a).[11] In principle, dinuclear complexes should be convenient platforms to build metal-coordinated metallabenzenes;[12]in fact, unsaturated hydrocarbyl ligands, when bridging coordinated, may exhibit a peculiar reactivity provided by cooperative effects typical of a bimetallic system, thus facilitating coupling reactions with small molecular fragmentsotherwise not viable on related monometallic species.[13]To the best of our knowledge, only a few ruthenabenzenes coordinated to a second ruthenium centre have been prepared to date starting from a poly-ruthenium framework,[14] neverthelessthe reported synthetic procedures suffer from poor selectivity and a narrow scope.[15,16]Specifically, Girolami and co-workers obtained an unsubstituted ruthenabenzene η^6-bound to $\{RuCp^*\}$, via double C-C coupling between two molecules of acetylene and a methylidene ligand bridging coordinated in the diruthenium precursor (Scheme 1b).[15] Bruce and co-workers isolated in 10% yield a ruthenium-coordinated bis-ferrocenyl ruthenabenzene, from the assembly of two alkyne molecules and an allenylidene ligandcoordinated in a triruthenium cluster according to the $\{\mu^3\text{-}\eta^1\text{:}\eta^1\text{:}\eta^2\}$ fashion (Scheme 1c).[16]

In the framework of our longtime research devoted to the construction of organometallic architectures on $\{M_2Cp_2(CO)_x\}$ scaffolds (M = Fe, Ru; x = 1-3),[17] our investigation on the reactivity with alkynes of a diruthenium complex containing a $\mu\text{-}\eta^1\text{:}\eta^2$-allenyl ligand led us to disclose a straightforward three-

component reaction yielding a ruthenium-coordinated ruthenabenzene motif.Our multi-technique study is described in the following.

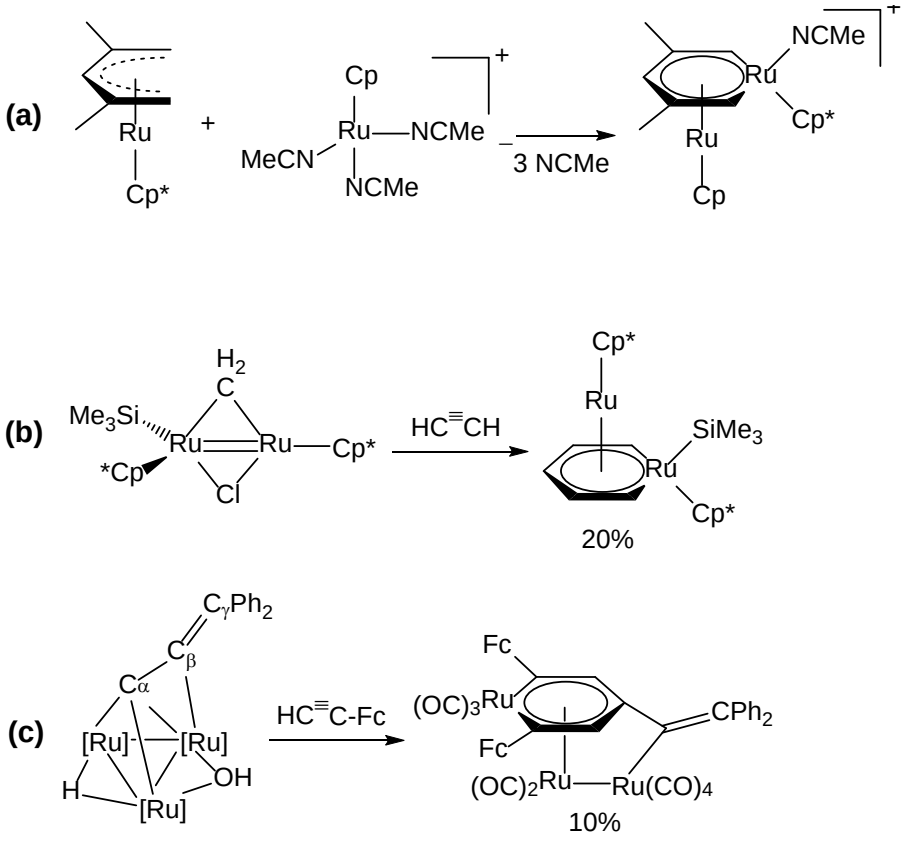

Scheme 1. Synthetic procedures from the literature to access ruthenium-coordinated ruthenabenzenes: a) example of ring closure reaction involving two monometallic precursors; b-c) coupling reactions of bridging hydrocarbyl ligands with alkynesin diruthenium complexes ([Ru] = $Ru(CO)_3$).

Results and discussion

The diruthenium μ-allenyl complex $[Ru_2Cp_2(CO)_3\{\mu\text{-}\eta^1\text{:}\eta^2\text{-}C^1H{=}C^2{=}C^3Me_2\}]BF_4$, **1**, was synthesized according to the published procedure.[18] This compound is unreactive towards alkynes and other unsaturated molecules, while the addition of nucleophiles bearing some basic character (e.g. amines, $NaBH_4$, lithium alkyls) is hampered by the acidity of the C^2H hydrogen, resulting in the quantitative deprotonation of the allenyl ligand.[19] Nonetheless, the substitution of one carbonyl ligand with acetonitrile is a convenient strategy to favor the addition to the allenyl of small units (i.e., hydride,[20]carbene[19] and alkenes[18]). This is viable by allowing **1** to react with trimethylamine-N-oxide

in the presence of acetonitrile.[21] The formation of $[Ru_2Cp_2(CO)_2(NCMe)\{\mu\text{-}\eta^1\text{:}\eta^2\text{-}C^1H{=}C^2{=}C^3Me_2\}]BF_4$, **1-NCMe**, takes place straightforwardly and the labile nitrile ligand is almost the equivalent for a vacant coordination site. Hence, the freshly prepared **1-NCMe** was investigated for its reactivity with alkynes. The room temperature reactions of **1-NCMe**with a series of symmetrical internal alkynes afforded the air-stable products **2-4**, which were isolated after work-up in high yields (Scheme 2).

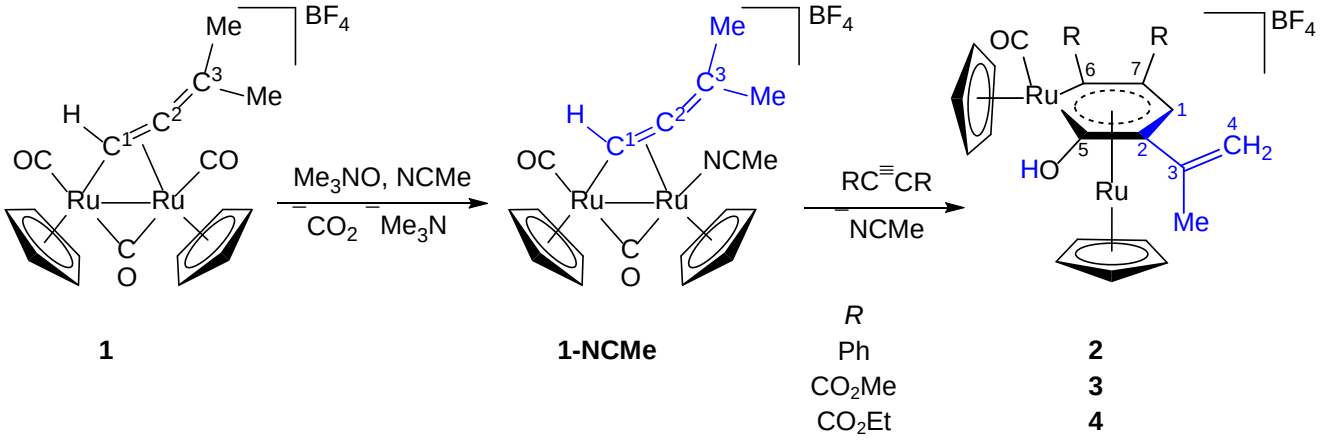

1 **1-NCMe**

R	
Ph	**2**
CO_2Me	**3**
CO_2Et	**4**

Scheme 2. Room temperature three-component coupling involving a bridging allenyl ligand, a carbonyl ligand and an alkyne reagent in a diruthenium complex, via preliminary carbon monoxide-acetonitrile replacement.

After several attempts, X-ray quality crystals were collected for **2** by a slow diffusion technique, and therefore the structure of this compound could be ascertained by X-ray diffraction (Figure 1 and Table 1). The quality of the crystals was very low and, in addition, there was extensive disosder in the cation. Thus, the cation was refined isotropically in order to avoid inappropriate isotropic restraints on anisotropic displacement parameters. The cation of **2** may be described as a ruthenabenzene, incorporating Ru(1), that is η^6-coordinated to Ru(2). Both ruthenium atoms are further bonded to a η^5-Cp ligand, and a terminal CO ligand is coordinated to Ru(1). The *cis*-Ru_2Cp_2 core, present in the parent complex **1**, is retained in **2**. The quality of the crystal is not very high[22] and, thus, bonding distances cannot be deeply discussed, however, they appear similar to those previously reported in the literature for η^6-coordinated ruthenabenzenes.[11a,14,15] Thus, distances between Ru(2) and the ring carbons fall in

the interval 2.053(18) - 2.254(18) Å; the C–C bonds within the six-membered ring [1.35(3) - 1.44(3) Å] display some π-character and also the C(5)–O(2) contact [1.31(2) Å] is shorter than a single bond. The Ru(1)–C(5) [2.053(18) Å] distance is somehow in the middle between Ru^{II}-(hydroxyl)alkylidene and Ru^{II}-alkyl bonds,[23] and Ru(1)–C(6) [2.08(2) Å] appears significantly elongated compared to pure Ru^{II}-alkylidene bonds.[24] A hydrogen bond is present between the OH group of the cation and one fluorine of the $[BF_4]^-$ anion [O(2)–H(2) 0.84 Å, H(2)···F(4) 2.14 Å, O(2)···F(4) 2.727(19) Å, <O(2)H(2)F(4) 126.4°]. The Ru–Ru distance [2.728(2) Å] is in keeping with Ru–Ru bonding contacts not supported by μ-CO ligands, as recognized in dinuclear complexes and polymetallic clusters.[25]

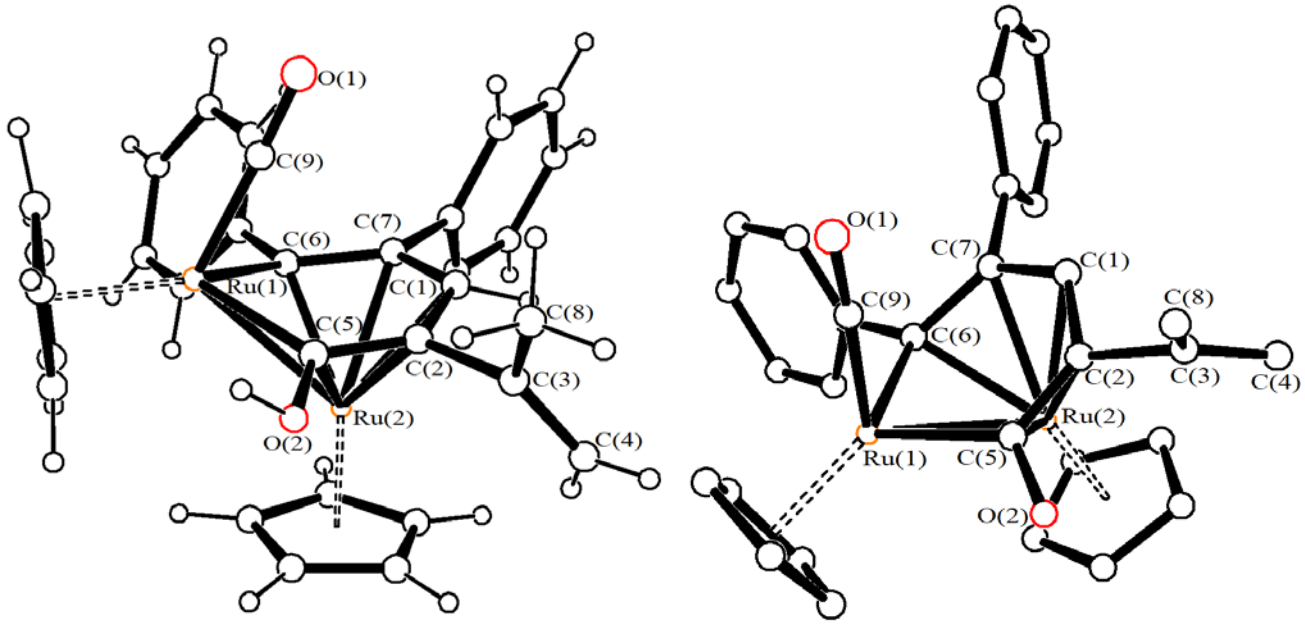

Figure 1. Two views of the molecular structure of the cation of **2**. H-atoms have been included only in one representation of the structure.

Table 1. Main bond distances (Å) and angles (°) of **2**.

Ru(1)–Ru(2)	2.728(2)	Ru(2)–C(5)	2.230(18)
Ru(2)–C(2)	2.18(2)	Ru(2)–C(1)	2.254(18)
Ru(2)–C(7)	2.227(18)	Ru(2)–C(6)	2.147(19)
Ru(1)–C(5)	2.053(18)	Ru(1)–C(6)	2.08(2)
C(5)–C(2)	1.35(3)	C(6)–C(7)	1.45(3)
C(2)–C(1)	1.42(3)	C(7)–C(1)	1.44(3)

Ru(1)–Cp_{av}	2.24(7)	Ru(2)–Cp_{av}	2.20(4)
Ru(1)–C(9)	1.836(18)	C(9)–O(1)	1.15(2)
C(5)–O(2)	1.31(2)	C(2)-C(3)	1.54(3)
C(3)–C(4)	1.33(3)	C(3)–C(8)	1.47(3)
C(5)–Ru(1)–C(6)	93.2(7)	Ru(1)–C(5)–C(2)	121.5(14)
C(5)–C(2)–C(1)	128.3(19)	C(2)–C(1)–C(7)	125.4(18)
C(1)–C(7)–C(6)	125.0(18)	C(7)–C(6)–Ru(1)	118.1(14)
C(2)–C(3)–C(4)	122.6(19)	C(2)–C(3)–C(8)	115.7(18)

The geometry of the cation of **2** was optimized by DFT calculations (Figure S1), revealing a good agreement with the experimental X-ray data (RMSD 0.242 Å).

The IR spectra of **2-4** (recorded in CH_2Cl_2 solution) exhibit one intense band related to one terminal carbonyl ligand, occurring at 2011 cm^{-1} in the case of **2** and at a higher wavenumber (2027 cm^{-1}) for **3** and **4**; this trend agrees with the electron-withdrawing nature of the carboxylato substituents, weakening the ruthenium to CO back-donation in **3** and **4**. In addition, the carboxylato moieties manifest themselves with an intense absorption around 1730 cm^{-1} in the IR spectra of **3** and **4**. The hydroxyl group was detected in the solid state spectrum of **2** as a broad band at 3448 cm^{-1}.

The NMR spectra of **2-4** (in acetone-d_6 solution) consist of single sets of resonances. The two cyclopentadienyls give rise to two singlets [*e.g.* for **2**: $\delta(^1H)$ = 5.89, 5.73 ppm] at chemical shifts resembling those reported for **1** [$\delta(^1H, CDCl_3)$ = 5.86, 5.64 ppm]; this data suggests that the Cp rings maintain the mutual cis configuration, with respect to the Ru–Ru axis, ongoing from **1** to **2-4**, in agreement with the X-ray evidence collected for **2**. In the $^{13}C\{^1H\}$ NMR spectra, the five carbons constituting the ruthenabenzene ring were recognized at 94.8-97.5 ppm (C^1), 77.7-101.7 ppm (C^2), 210.2-213.1 ppm (C^5), 174.5-188.2 ppm (C^6) and 103.6-114.2 ppm (C^7). In particular, the low field resonances attributed to the ruthenium bound carbons (i.e., C^5 and C^6) highlight their alkylidene nature, consistently with the partial double bond character of the Ru–C connections detected on **2** by X-ray diffraction. The carbonyl ligand produces a resonance at 197.7-200.0 ppm, confirming the terminal

coordination mode shown by IR and X-ray data. The resonances related to the $\{C^3CH_2\}$ moiety are clearly indicative of an alkenic nature; more precisely, protons resonate as two multiplets centred around 5.2 and 5.4 ppm, while the two carbons occur at ca. 199 and 143 ppm in the ^{13}C spectra. The $^{19}F\{^1H\}$ NMR spectra of **2-4** consist in two close resonances around 150 ppm, attributable to $^{10}BF_4^-$ and $^{11}BF_4^-$, respectively.

The aromaticity of the ruthenabenzene ring in **2** was investigated by DFT calculations. The five carbon atoms of the ruthenabenzene have similar Hirshfeld partial charges, included in the range –0.009 to–0.096 a.u. (see Figure S1), thus indicating that the electron density is quite homogeneously distributed. Then, the Shannon aromaticity index (SA) was calculated based on the C–C and C–Ru bond critical points (b.c.p.), obtained from the *Atom-in Molecules* (AIM) analysis of the DFT-optimized structure.[26]SA waschoseninstead of the NICS (nucleus-independentchemical shifts) approach[27]sincethe formeronlydependsupon the electron densityatb.c.p., while NICS requires the localization of the ring centre and differentdefinitions of NICS are present in the literature. Moreover, NICS dependsupon the magneticshieldingtensor and itistherefore more sensitive to the computationalmethodused. The SA of $\{RuC_5\}$ resulted$5\cdot10^{-2}$, a value in line with those calculated at the same theoretical level for other ruthenabenzene rings η^6-coordinated to a second ruthenium centre. In particular, SA of $4\cdot10^{-2}$ was obtained for $[Ru_2Cp^*_2(SiMe_3)(\mu\text{-}\eta^2\text{:}\eta^5\text{-}C_5H_5)]$ (Cp^* =η^5-C_5Me_5, Scheme 1b),[15] while the SA value for the ruthenabenzene in $[Ru_3(CO)_9\{\mu_3\text{-}(FcCCH)_2CC{=}CPh_2\}]$ (Fc = ferrocenyl, Scheme 1c) is $7\cdot10^{-2}$.[16] The DFT-optimized structures of these literature compounds and the RMS deviations with respect to the corresponding X-ray data are shown in Figure S2. In all cases, the SA values are higher than the $3\cdot10^{-3}$- $5\cdot10^{-3}$ limit suggested for classical aromatic compounds; metallabenzenes are commonly considered to be aromatic even though the aromatic stabilization is considerably weaker than that of conventional arenes.[3] The AIM analysis on **2**was unable to find b.c.p. between the two ruthenium atoms, indicating lack of a significantly localized metal-metal orbital

overlapping. Moreover, no b.c.p. was found between Ru2 and C7. The density (ρ) and potential energy density (V) values obtained for the b.c.p. between Ru2 and the ruthenabenzene carbon are not strictly homogeneous (Table S1), and show that the strongest interaction occurs between Ru2 and C6.

The synthetic study was extended to the exploration of the reactivity of **1-NCMe** with a few terminal alkynes. Unfortunately, these reactions did not take place selectively and will not be discussed further.

It appears reasonable that the synthesis of **2-4** from **1-NCMe** proceeds with initial acetonitrile displacement by the alkyne molecule reagent, followed by fast insertion of the latter into the Ru-C^1 bond. The cyclization process affording the final ruthenabenzene ring incorporates one of the two carbonyl ligands, coupling with the central atom (C^2) of the original allenyl chain, and includes a hydrogen migration event (from CH_3 to oxygen). Previous examples of allenyl-alkyne coupling were described by Doherty and co-workers on a diiron system[28] and by Carty on a diruthenium complex involving also a carbonyl ligand.[29]Adams reported an allene-alkyne combination on an osmium cluster,[30] while the trimethylamine adduct [$Fe(CO)_4(NMe_3)$] was found to promote allenyl/alkyne/CO coupling.[31] However, the three-component assembly depicted in Scheme 2 is unique in the landscape of the chemistry of allenyl complexes.

Since metallabenzenes are prone to undergo nucleophilic attack,[32] and on account of the cationic nature of **2-4**, we moved to explore the chemistry of these complexes with nucleophiles. However, the reactions of **2-4** with a variety of nucleophiles ($NaBH_4$, lithium acetylides, lithium alkyls) highlighted the acidic character of the hydroxyl group and resulted in deprotonation. Triethylamine revealed the best choice to perform the deprotonation reaction, thus the neutral complexes **5-7** were isolated in very good yields as air-stable solid materials, following alumina chromatography (Scheme 3). The proton removal is reversible, in that the addition of tetrafluoroboric acid to dichloromethane solutions of **5-7** led to the selective recovery of **2-4** (see Experimental for details).

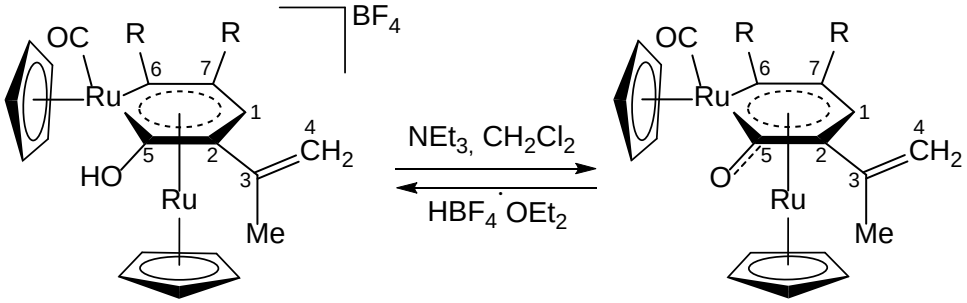

	R	
2	Ph	**5**
3	CO_2Me	**6**
4	CO_2Et	**7**

Scheme 3. Reversible deprotonation of the hydroxyl substituent on ruthenabenzene.

We could not obtain X-ray quality crystals of one representative compound of the series **5-7**. However, the structure of **5** was optimized by DFT calculations, and a view of this structure is shown in Figure 2; selected computed bond lengths of $[\mathbf{2}]^+$ and **5** are compared in Table 2.

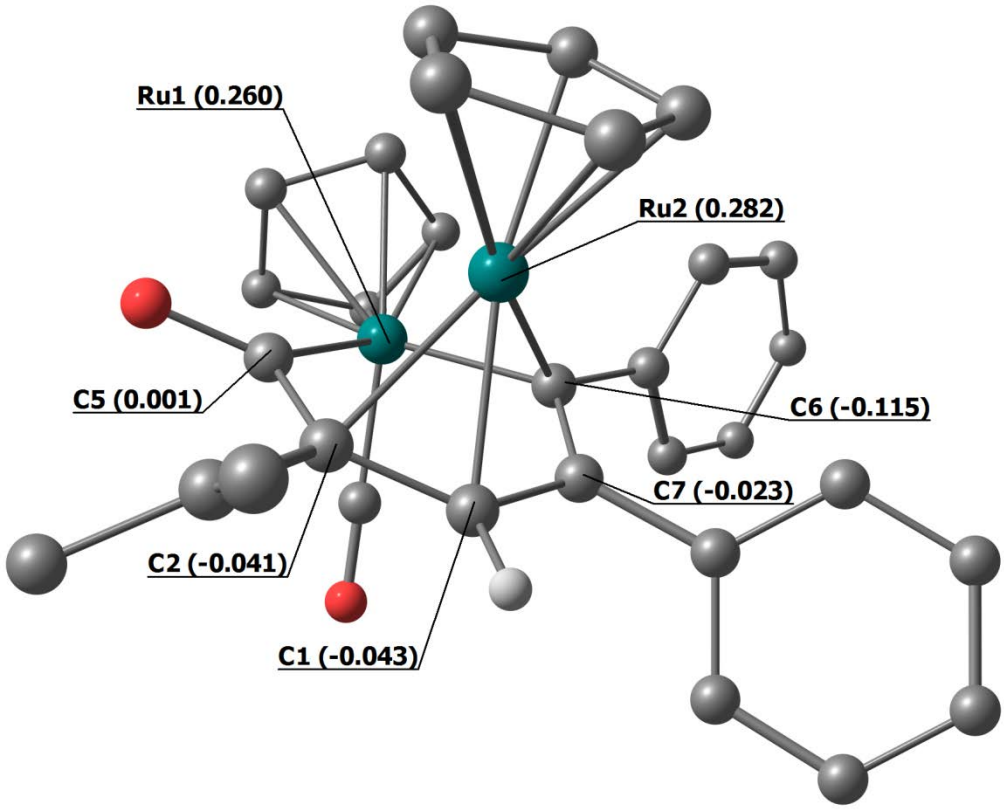

Figure 2. View of the DFT-optimized structure of **5**. Selected Hirshfeld partial charges (a.u.) in parenthesis. Colour map: Ru, dark green; O, red; C, grey. Hydrogen atoms, except that of the ruthenabenzene ring, are omitted for clarity.

Table 2. Selected computed distances (Å) for [**2**]$^+$ and **5**.

	[2]$^+$	5		[2]$^+$	5
Ru1–C6	2.046	2.051	Ru2–C7	2.219	2.207
C6–C7	1.428	1.426	Ru2–C1	2.195	2.192
C7–C1	1.432	1.436	Ru2–C2	2.219	2.227
C1–C2	1.425	1.418	Ru2–C5	2.186	2.404
C2–C5	1.438	1.482	Ru1–Cp(average)	2.270	2.284
C5–Ru1	2.005	2.039	Ru1–C(CO)	1.870	1.846
Ru1⋯Ru2	2.754	2.774	Ru2–Cp(average)	2.196	2.189
Ru2–C6	2.151	2.128	C5–O	1.347	1.235

DFT calculations ruled out that deprotonation of **2-4** could involve the ruthenabenzene hydrogen ratherthan the OH group, the related product being 51.1 kcal mol^{-1} less stable than **5** (see also Figure S3 for a comparative view of the two isomers). The deprotonation of the hydroxyl group scarcely affects the structure of the complex, being the RMSD between computed **5** and [**2**]$^+$ (except for the hydroxyl hydrogen) only 0.332 Å. However, the bond between C5 and Ru2 undergoes a considerable elongation on moving from [**2**]$^+$ to **5**, suggesting a reduced coordination ability of the {C=O} carbon with respect to {C–OH}. Despite the calculated SA index of the ruthenabenzene in **5** is identical to that of [**2**]$^+$ ($5\cdot10^{-2}$), the Hirshfeld partial charges of the carbon atoms are spanned over a wider range (from0.001 to–0.115 a.u.), essentially due to the increased electron density on C[1]. As for [**2**]$^+$, also in **5** the AIM analysis did not revealb.c.p. between the two metal centres. On the other hand, b.c.p. was found for the Ru2–C6, Ru2–C1 and Ru2–C2 couples of attractors. On the basis of the ρ and V values at b.c.p. (Table 3), the strongest interaction between Ru2 and the ruthenacene occurs through C6, in agreement with the marked nucleophilicity of this carbon as deduced from the Hirshfeld distribution.

Table 3. Density (ρ) and potential energy density (V) values (a.u.) for selected b.c.p. in **5**.

Bond	ρ	V
Ru2-C6	0.099	-0.121
Ru2-C1	0.082	-0.104
Ru2-C2	0.079	-0.093

On account of the DFT outcomes, two main resonance forms seem to significantly contribute to the structure of **5** (Figure 3), the form **B** accounting for the ruthenabenzene character.

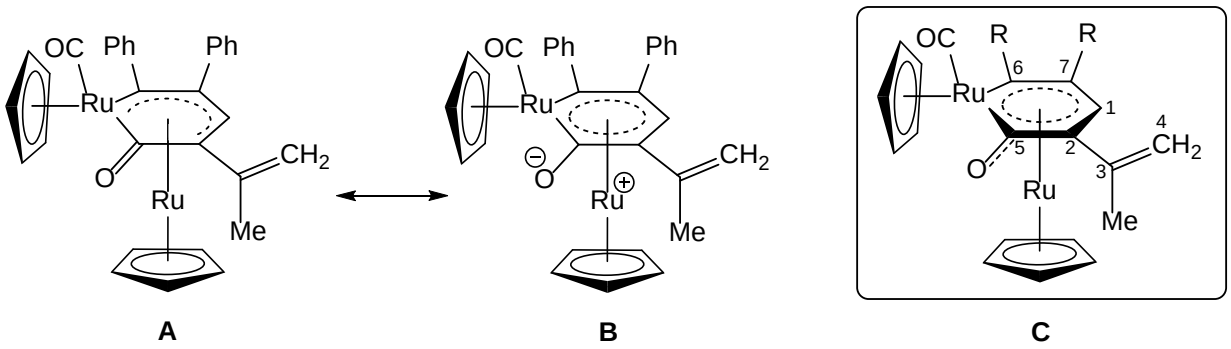

Figure 3. Resonance forms representing the structure of **5** (**A** and **B**), and combined representation with delocalized charge (**C**).

Spectroscopic data of **5-7** are in accordance with the structural features provided by the theoretical study regarding **5**. Thus, the IR spectra (in CH_2Cl_2 solution) display one absorption ascribable to the terminal carbonyl ligand, which is ca. 50 cm^{-1} shifted to lower wavenumbers compared to what detected for **2-4**, as a consequence of the loss of the net positive charge on going from **2-4** to **5-7**. Compared to the related spectrum of the parent complex **2**, the solid state IR spectrum of **5** lacks the OH absorption; instead, an intense band at 1594 cm^{-1} accounts for the C^5-O function, bearing a partial double bond character. The NMR spectra of **5-7** (in $CDCl_3$) display single sets of resonances which are quite close to those recognized for the corresponding precursors**2-4**, confirming that the reversible H^+ elimination/addition occurs with small structural variations. For instance, the ^{13}C resonances for the ruthenabenzene moiety in compound **6**have been detected at 94.3 (C^1), 75.9 (C^2), 145.9 (C^3), 116.4

(C^4), 213.5 (C^5), 166.9 (C^6) and 89.4 (C^7) ppm, while the respective resonances in the parent compound**3** fall at94.8, 77.4, 143.1, 119.3, 213.1, 175.1 and 94.8 ppm, in the order given.

Conclusions.

Metallabenzenes constitute a widely investigated class of organometallic compounds, and the development of novel synthetic methods is currently of great interest. With specific reference to ruthenium, a variety of ruthenabenzenes has been reported, including ruthenabenzenes acting as six-membered cyclic ligands towards a second metal centre. Among the routes giving access to ruthenium-coordinated ruthenabenzenes, the modification of a suitable, bridging hydrocarbyl ligand in a diruthenium precursor is a potentially versatile strategy, taking advantage of the cooperative effects arising from the bimetallic core, but substantially undeveloped so far. Using this approach, we have found that aunprecedented three component reaction, involving CO, the μ-allenyl ligand and an external alkyne reagent, is a straightforward method to obtain η^6-coordinated ruthenabenzenes. X-ray and DFT analyses revealed a degree of aromaticity comparable to that of related literature compounds.

Experimental

Materials and methods. Reactants and solvents were purchased from Alfa Aesar, Merck, Strem or TCI Chemicals, and were of the highest purity available. Complex **1**was prepared according to the literature procedure.[18]Reactions were conducted under N_2 atmosphere using standard Schlenk techniques, and all products were stored in air once isolated. Dichloromethane and diethyl ether were dried with the solvent purification system mBraun MB SPS5, while acetonitrile was distilled from CaH_2. IR spectra of solutions were recorded using a CaF_2 liquid transmission cell (2300-1500 cm^{-1}) on a Perkin Elmer Spectrum 100 FT-IR spectrometer. IR spectra of solid samples were recorded on an Agilent Cary630 FTIR spectrometer. IR spectra were processed with Spectragryph software.[33] NMR spectra were

recorded at 298 K on a Jeol JNM-ECZ500R instrument equipped with a Royal HFX Broadband probe. Chemical shifts (expressed in parts per million) are referenced to the residual solvent peaks (^{1}H, ^{13}C)[34] or to external standard (^{19}F to $CFCl_3$). ^{1}H and $^{13}C\{^{1}H\}$NMR spectra were assigned with the assistance of ^{1}H-^{13}C (*gs*-HSQC and *gs*-HMBC) correlation experiments.[35] Elemental analyses were performed on a Vario MICRO cube instrument (Elementar).

Reactions of 1 with alkynes: synthesis and characterization of $[Ru_2Cp_2(CO)_2\{\mu\text{-}\eta^2\text{:}\eta^5\text{-}C^6(R)C^7(R)C^1HC^2(C^3Me{=}C^4H_2)C^5(OH)\}]BF_4$ (R = Ph, 2; R = CO_2Me, 3; R = CO_2Et, 4).

General procedure. Complex **1** (*ca*. 0.30 mmol) was dissolved in CH_2Cl_2 (25 mL) and treated with a solution of Me_3NO in acetonitrile (1.0 eq. in 0.10 M solution). After 15 minutes stirring, the formation of the acetonitrile adduct **1-NCMe** was routinely checked by IR spectroscopy [IR (CH_2Cl_2): $\tilde{\upsilon}/cm^{-1}$ = 2003s (CO), 1853br-m (μ-CO)].[18,19] The volatiles were removed under vacuum to give a brown residue, which was dissolved in CH_2Cl_2 (25 mL). The selected alkyne (ca. 5 eq.) was added to this solution. The resulting mixture was stirred overnight at room temperature, the solvent was removed under reduced pressure, and the obtained residue was washed with Et_2O (3 x 15 mL) and dried under vacuum.

$[Ru_2Cp_2(CO)_2\{\mu\text{-}\eta^2\text{:}\eta^5\text{-}C^6(Ph)C^7(Ph)C^1HC^2(C^3Me{=}C^4H_2)C^5(OH)\}]BF_4$, 2 (Figure 4).

Figure 4. Structure of **2**.

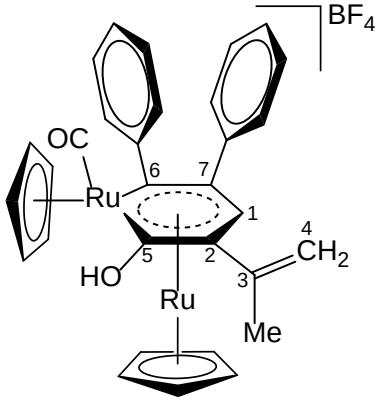

From **1** (162 mg, 0.284 mmol), Me_3NO and diphenylacetylene (175 mg, 0.980 mmol). Pale orange solid, yield 192 mg (94%). Anal. calcd. For $C_{31}H_{27}BF_4O_2Ru_2$: C, 51.68; H, 3.78; Found: C, 51.59; H, 3.88. IR (CH_2Cl_2): $\tilde{\upsilon}/cm^{-1}$ = 2011 (CO). IR (solid state): $\tilde{\upsilon}/cm^{-1}$ = 3448m-br (OH), 1985vs (CO). ^1H NMR (acetone-d_6): δ/ppm = 7.38, 7.27, 7.15-7.10, 7.06-7.02, 6.77 (m, 10 H, Ph); 6.01 (m,1 H, C^1H); 5.89, 5.73 (s, 10 H, Cp); 5.43, 5.26 (m, 2 H, C^4H_2); 3.15 (br, 1 H, OH); 2.23 (m, 3 H, C^3Me). $^{13}C\{^1H\}$ NMR (acetone-d_6): δ/ppm = 210.2 (C^5); 200.0 (CO); 188.2 (C^6); 152.9, 139.9 (ipso-Ph); 143.9 (C^3); 131.3, 129.1, 128.8, 128.6, 128.4, 128.3, 128.0, 126.7 (Ph); 119.2 (C^4); 114.2 (C^7); 101.7 (C^2); 97.5 (C^1); 96.8, 87.5 (Cp); 23.0 (C^3*Me*).$^{19}F\{^1H\}$ NMR (acetone-d_6): δ/ppm = −150.0 ($^{11}BF_4^-$), −149.9 ($^{10}BF_4^-$). Crystals for X-ray analysis were collected by slow diffusion of diethyl ether into a dichloromethane solution of **2** at room temperature.

$[Ru_2Cp_2(CO)_2\{\mu\text{-}\eta^2\text{:}\eta^5\text{-}C^6(CO_2Me)C^7(CO_2Me)C^1HC^2(C^3Me{=}C^4H_2)C^5(OH)\}]BF_4$, 3 (Figure 5).

Figure 5. Structure of **3**.

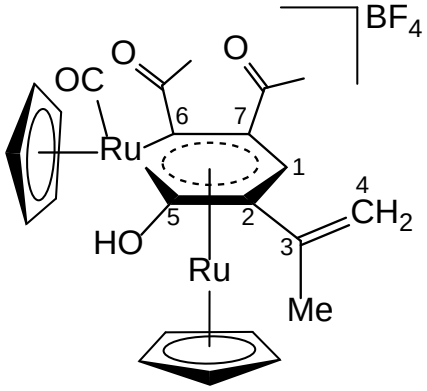

From **1** (194 mg, 0.340 mmol), Me_3NO and dimethylacetylenedicarboxylate (0.20 mL, 1.63 mmol). Orange solid, yield 193 mg (83%). Anal. calcd. for $C_{23}H_{23}BF_4O_6Ru_2$: C, 40.37; H, 3.39. Found: C, 40.35; H, 3.34. IR (CH_2Cl_2): $\tilde{\upsilon}/cm^{-1}$ = 2027m (CO), 1738vs (C=O). ^1H NMR (acetone-d_6): δ/ppm = 6.38 (s,1 H, C^1H); 6.06, 5.69 (s, 10 H, Cp); 5.41, 5.16 (m, 2 H, C^4H_2); 3.88, 3.86 (s, 6 H, OMe); 2.15 (m, 3 H, C^3Me); OH not observed.$^{13}C\{^1H\}$ NMR (acetone-d_6): δ/ppm = 213.1 (C^5); 197.7 (CO); 175.1 (C^6); 174.4, 168.4 (OCO); 143.1 (C^3); 119.3 (C^4); 103.6 (C^7); 96.2, 88.8 (Cp); 94.8 (C^1); 77.7 (C^2); 54.2, 53.2 (OMe); 23.4 (C^3*Me*). $^{19}F\{^1H\}$ NMR (acetone-d_6): δ/ppm = –149.85 ($^{11}BF_4^-$), –149.79 ($^{10}BF_4^-$).

$[Ru_2Cp_2(CO)_2\{\mu\text{-}\eta^2\text{:}\eta^5\text{-}C^6(CO_2Et)C^7(CO_2Et)C^1HC^2(C^3Me{=}C^4H_2)C^5(OH)\}]BF_4$, 4 (Figure 6).

Figure 6. Structure of **4**.

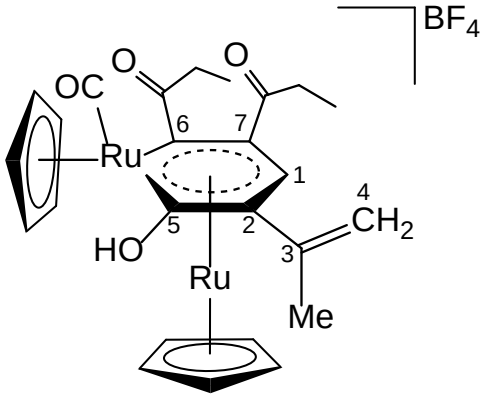

From **1** (183 mg, 0.321 mmol), Me_3NO and diethylacetylenedicarboxylate (0.20 mL, 1.25 mmol). Orange solid, yield 197 mg (86%). Anal. calcd. for $C_{25}H_{27}BF_4O_6Ru_2$: C, 42.15; H, 3.82. Found: C, 42.25; H, 3.75. IR (CH_2Cl_2): $\tilde{\upsilon}/cm^{-1}$ = 2027m (CO), 1722vs (C=O). ^1H NMR (acetone-d_6): δ/ppm = 6.37 (s,1 H, C^1H); 6.06, 5.69 (s, 10 H, Cp); 5.41, 5.17 (m, 2 H, C^4H_2); 4.35 (m, 4 H, OCH_2); 2.15 (s, 3 H, C^3Me); 1.39, 1.33 (t, $^3J_{HH}$ = 7.2 Hz, 6 H, $CH_2C\mathit{H}_3$); OH not observed. $^{13}C\{^1H\}$ NMR (acetone-d_6): δ/ppm = 212.9 (C^5); 197.8 (CO); 174.5 (C^6); 174.5, 167.9 (OCO); 143.1 (C^3); 119.3 (C^4); 103.7 (C^7); 96.2, 88.8 (Cp); 94.8 (C^1); 77.7 (C^2); 63.8, 62.6 (OCH_2); 23.4 ($C^3\mathit{Me}$); 14.6, 14.3 ($CH_2\mathit{C}H_3$). $^{19}F\{^1H\}$ NMR (acetone-d_6): δ/ppm = –149.9 ($^{11}BF_4^-$), –149.8 ($^{10}BF_4^-$).

Deprotonation reaction of 2-4: synthesis and characterization of $[Ru_2Cp_2(CO)_2\{\mu\text{-}\eta^2\text{:}\eta^5\text{-}C^6(R)C^7(R)C^1HC^2(C^3Me{=}C^4H_2)C^5(O)\}]$ (R = Ph, 5; R = CO_2Me, 6; R = CO_2Et, 7).

The selected complex **2-4** (*ca*. 0.15 mmol) was dissolved in CH_2Cl_2 (15 mL) and treated with an excess (5-8 eq.) of NEt_3. The mixture was stirred for 4 hours, and then directly charged on top of an alumina column. Elution with CH_2Cl_2 allowed to separate impurities, then the fraction corresponding to the title compound was eluted using neat THF.The solvent was removed under reduced pressure and the residue was washed with pentane (2 x 10 mL) and then dried under vacuum.

$[Ru_2Cp_2(CO)_2\{\mu\text{-}\eta^2\text{:}\eta^5\text{-}C^6(Ph)C^7(Ph)C^1HC^2(C^3Me{=}C^4H_2)C^5(O)\}]$, 5 (Figure 7).

Figure 7. Structure of **5**.

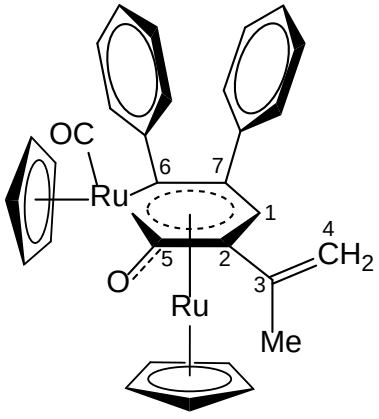

From **2** (108 mg, 0.150 mmol) and triethylamine (0.11 mL, 0.80 mmol). Red solid, yield 84 mg (88%). Anal. calcd. For $C_{31}H_{26}O_2Ru_2$: C, 58.85; H, 4.14; Found: C, 58.79; H, 4.18. IR (CH_2Cl_2): ϋ/cm^{-1} = 1965 (CO). IR (solid state): ϋ/cm^{-1} = 1955 (CO), 1594 (CÓO). ^{1}H NMR ($CDCl_3$): δ/ppm = 7.09-7.07, 7.05-7.02, 6.93-6.90 (m, 10 H, Ph); 5.72 (s,1 H, C^1H); 5.19, 5.06 (m, 2 H, C^4H_2); 5.10, 5.09 (s, 10 H, Cp); 2.12 (m, 3 H, C^3Me). $^{13}C\{^1H\}$ NMR ($CDCl_3$): δ/ppm = 214.7 (C^5); 203.0 (CO); 178.2 (C^6); 154.5, 142.1 (ipso-Ph); 146.8 (C^3); 130.4, 127.4, 127.1, 126.7, 124.7 (Ph); 116.1 (C^4); 112.2 (C^7); 96.9 (C^1); 94.5, 81.9 (Cp); 73.7 (C^2); 22.8 (C^3*Me*).

[$Ru_2Cp_2(CO)_2\{\mu$-η^2:η^5-$C^6(CO_2Me)C^7(CO_2Me)C^1HC^2(C^3Me{=}C^4H_2)C^5(O)\}$], 6 (Figure 8).

Figure 8. Structure of **6**.

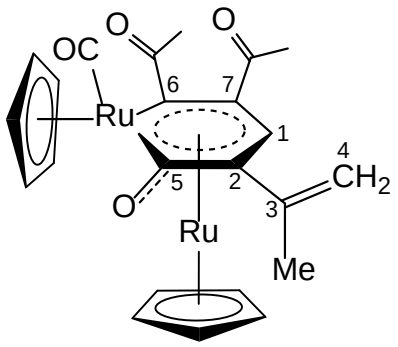

From **3** (96 mg, 0.14 mmol) and triethylamine (0.12 mL, 0.84 mmol). Pale red solid, yield 68 mg (81%). Anal. calcd. For $C_{23}H_{22}O_6Ru_2$: C, 46.31; H, 3.72; Found: C, 46.39; H, 3.78. IR (CH_2Cl_2): ϋ/cm^{-1} = 1981vs (CO), 1741s (C=O), 1725s (C=O), 1605 (CÓO). ^{1}H NMR ($CDCl_3$): δ/ppm = 6.23 (s,1 H, C^1H); 5.34, 5.02 (s, 10 H, Cp);5.17, 4.70 (m, 2 H, C^4H_2); 3.84, 3.81 (s, 6 H, OMe); 2.05 (m, 3 H, C^3Me). $^{13}C\{^1H\}$ NMR ($CDCl_3$): δ/ppm = 213.5 (C^5); 200.2 (CO); 177.7, 170.4 (OCO); 166.9 (C^6); 145.9 (C^3); 116.4 (C^4); 94.3 (C^1); 93.8, 82.9 (Cp); 89.4 (C^7); 75.9 (C^2); 53.2, 52.3 (OMe); 23.1 (C^3*Me*).

[$Ru_2Cp_2(CO)_2\{\mu$-η^2:η^5-$C^6(CO_2Et)C^7(CO_2Et)C^1HC^2(C^3Me{=}C^4H_2)C^5(O)\}$], 7 (Figure 9).

Figure 9. Structure of **7**.

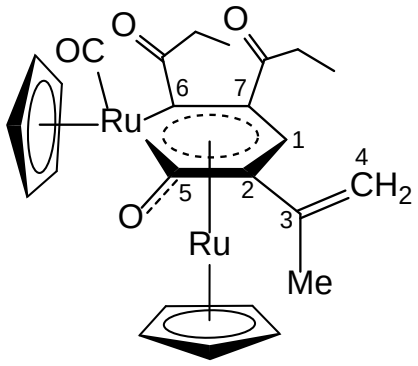

From **4** (108 mg, 0.152 mmol) and triethylamine (0.12 mL, 0.84 mmol). Red solid, yield 71 mg (75%). Anal. calcd. For $C_{25}H_{26}O_6Ru_2$: C, 48.07; H, 4.19; Found: C, 47.99; H, 4.26. IR (CH_2Cl_2): $\tilde{\upsilon}/cm^{-1}$ = 1982s (CO), 1712s (C=O), 1605 (CÓO). ^{1}H NMR ($CDCl_3$): δ/ppm = 6.21 (s,1 H, C^1H); 5.34, 5.01 (s, 10 H, Cp);5.17, 4.98 (m, 2 H, C^4H_2); 4.31-4.23 (m, 4 H, OCH_2); 2.06 (m, 3 H, C^3Me); 1.38-1.18 (m, 6 H, $CH_2C\mathit{H_3}$). $^{13}C\{^1H\}$ NMR ($CDCl_3$): δ/ppm = 213.6 (C^5); 200.2 (CO); 177.0, 169.9 (OCO); 167.2 (C^6); 151.7 (C^3); 116.3 (C^4); 94.3 (C^1); 93.8, 82.9 (Cp); 90.1 (C^7); 75.9 (C^2); 62.2, 60.9 (OCH_2); 30.4 ($C^3\mathit{Me}$); 14.7, 14.4 ($CH_2\mathit{C}H_3$).

Formation of 2-4 by protonation of 5-7.

Complex**5** (51 mg, 0.080 mmol) was dissolved in CH_2Cl_2 (10 mL) and $HBF_4{\cdot}Et_2O$ (11 μL, 0.080 mmol) was added to this solution. The resulting solution was stirred for 15 minutes at room temperature, then the volume was concentrated up to ca. 3 mL and diethyl ether (30 mL) was added. The precipitate was filtered, washed with Et_2O (3 x 5 mL) and dried under vacuum affording **2** as a microcrystalline solid. Yield 48 mg (83%). The same procedure allowed to obtain compounds **3** (78% yield) and **4** (81% yield) from **6** and **7**, respectively.

X-ray crystallography

Crystal data and collection details for **2** are reported in Table 4. Data were recorded on a Bruker APEX II diffractometer equipped with a PHOTON2 detector using Mo–Kα radiation. The structure was

solved by direct methods and refined by full-matrix least-squares based on all data using F^2.[36] Hydrogen atoms were fixed at calculated positions and refined using a riding model. The quality of the crystals was very low and, in addition, there was extensive disosder in the cation. Thus, the cation was refined isotropically in order to avoid inappropriate isotropic restraints on anisotropic displacement parameters.

Table 4. Crystal data and measurement details for **2**.

	2
Formula	$C_{31}H_{27}BF_4O_2Ru_2$
FW	720.47
T, K	100(2)
λ, Å	0.71073
Crystal system	Orthorhombic
Space group	*Pbca*
a, Å	9.7307(19)
b, Å	18.031(4)
c, Å	31.013(6)
Cell Volume, Å^3	5441.5(19))
Z	8
D_c, g·cm^{-3}	1.759
μ, mm^{-1}	1.166
F(000)	2864
Crystal size, mm	0.19×0.16×0.08
θ limits,°	2.259-25.050
Reflections collected	39820
Independent reflections	4817 [R_{int} = 0.1066]
Data / restraints /parameters	4817 / 0 / 188
Goodness on fit on F^2	1.165
R_1 ($I > 2\sigma(I)$)	0.1521
wR_2 (all data)	0.3520
Largest diff. peak and hole, e Å^{-3}	5.935 / –7.357

DFT calculations

The ground-state structures were optimized using the the range-separated hybrid ωB97X DFT functional [37] in combination with Ahlrichs' split-valence-polarized basis set and relativistic ECP

including 28 core electrons for Ru.[38] The C-PCM implicit solvation model was added to ωB97X calculations, considering dichloromethane as continuous medium.[39] The stationary points were characterized by IR simulations (harmonic approximation), from which zero-point vibrational energies and thermal corrections (T = 25 °C) were obtained. The software used was Gaussian 09.[40] Hirshfeld and AIM analyses were carried out using MultiWFN, version 3.5.[41] Cartesian coordinates of the DFT-optimized structures are collected in a separated .xyz file.

Author contributions

Conceptualization, G.B., S.Z., G.P., M.B., F.M.; Data curation, G.B., S.Z., M.B., F.M.; Formal Analysis, G.B., S.Z., G.P., M.B., F.M.; Funding acquisition, G.P., F.M.; Investigation Methodology, G.B., S.Z., M.B., F.M.; Supervision, G.P., F.M.; Validation, G.B., F.M.; Writing – original draft, G.B., S.Z., M.B., F.M.; Writing – review & editing, G.B., S.Z., G.P., M.B., F.M..

Conflict of interest

The authors declare no competing financial interest.

Acknowledgements

We thank the University of Pisa for financial support (Fondi di Ateneo 2021).

Supporting Information Available

DFT studies; NMR spectra of products. Cartesian coordinates of the DFT-optimized structures are collected in a separated .xyz file. CCDC reference number 2154982 (**2**) contains the supplementary crystallographic data for the X-ray study reported in this work. This data is available free of charge at http://www.ccdc.cam.ac.uk/structures.

References

1 D. L. Thorn, R. Hoffmann, Delocalization in metallocycles. Nouv. J. Chim. 1979, 3, 39-45.

2 H. Yamazaki, K.A. Aoki, Novel Six-Membered Ruthenium Metallocycle. J. Organomet. Chem. 1976, 122, C54-C58.

3 (a) I. Fernández, G. Frenking, Aromaticity in Metallabenzenes. 2007, 13, 5873-5884. (b) I. Fernandez, G. Frenking, G. Merino, Aromaticity of metallabenzenes and related compounds. Chem. Soc. Rev. 2015, 44, 6452-6463. (c) N. V. Tkachenko, A. Muñoz-Castro, A. I. Boldyrev, Occurrence of Double Bond in π-Aromatic Rings: An Easy Way to Design Doubly Aromatic Carbon-Metal Structures. Molecules 2021, 26, 7232.

4 (a) C. W. Landorf, M. M. Haley, Recent Advances in Metallabenzene Chemistry. Angew. Chem. Int. Ed. 2006, 45, 3914-3936. (b) J. R. Bleeke, Metallabenzenes. Chem. Rev. 2001, 101, 1205-1227.

5 (a) J. R. Bleeke, P. V. Hinkle, M. Shokeen, N. P. Rath, Metallacyclohexadiene and Metallabenzene Chemistry. Part 18. Synthesis, Structure, Spectroscopy, and Reactivity of a Neutral Iridathiabenzene. Organometallics 2004, 23, 4139-4149. (b) J. R. Bleeke, P. V. Hinkle, N. P. Rath, Metallacyclohexadiene and Metallabenzene Chemistry. Part 15. Synthesis, Structure, Spectroscopy, and Reactivity of a Metallathiabenzene. J. Am. Chem. Soc. 1999, 121, 595-596. (c) K. Masada, S. Kusumoto, K. Nozaki, Atom Swapping on Aromatic Rings: Conversion from Phosphinine Pincer Metal Complexes to Metallabenzenes Triggered by O_2 Oxidation. DOI: 10.1002/anie.202117096

6 D. Chen, Y. Hua, H. Xia, Metallaaromatic Chemistry: History and Development. Chem. Rev. 2020, 120, 12994-13086, and references therein.

7 S. Gupta, S. Su, Y. Zhang, P. Liu, D. J. Wink, D. Lee, Ruthenabenzene: A Robust Precatalyst. J. Am. Chem. Soc. 2021, 143, 7490-7500.

8 Yang, J.; Jones, W. M.; Dixon, J. K.; Allison, N. T. Detection of a Ruthenabenzene, Ruthenaphenoxide, and Ruthenaphenanthrene Oxide: The First Metalla Aromatics of a Second-Row Transition Metal. J. Am. Chem. Soc. 1995, 117, 9776-9777.

9 (a) G. R. Clark, T. R. O'Neale, W. R. Roper, D. M. Tonei, L. J. Wright, Stable Cationic and Neutral Ruthenabenzenes. Organometallics 2009, 28, 567-572. (b) H. Zhang, R. Lin, J. Li, J. Zhu, H. Xia, Interconversion between Ruthenacyclohexadiene and Ruthenabenzene: A Combined Experimental and Theoretical Study. Organometallics 2014, 33, 5606-5609.

10 (a) H. Zhang, H. Xia, G. He, T. B. Wen, L. Gong, G. Jia, Synthesis and Characterization of Stable Ruthenabenzenes. Angew. Chem. Int. Ed. 2006, 45, 2920-2923.

11 (a) U. Bertling, U. Englert, A. Salzer, From Triple-Decker to Metallabenzene: a new generation of sandwich complexes, Angew. Chem., Int. Ed. Engl., 1994, 33, 1003-1004). (b) U. Englert, F. Podewils, I. Schiffers, A. Salzer, The First Homoleptic Metallabenzene Sandwich Complex. Angew. Chem. Int. Ed. 1998, 37, 2134-2136. (c) U. Effertz, U. Englert, F. Podewils, A. Salzer, T. Wagner, M. Kaupp, Reaction of Pentadienyl Complexes with Metal Carbonyls: Synthetic, Structural, and Theoretical Studies of Metallabenzene π-Complexes. Organometallics 2003, 22, 264-274.

12 H. Tsurugi, P. Laskar, K. Yamamoto, K. Mashima, J. Organomet. Chem. 2018, 869, 251-263.

13 (a) Patra, S.; Maity, N. Recent advances in (hetero)dimetallic systems towards tandem catalysis. Coord. Chem. Rev. 2021, 434, 213803. (b) Ritleng, V.; Chetcuti, M. J. Hydrocarbyl Ligand Transformations on Heterobimetallic Complexes. Chem. Rev. 2007, 107, 797−858. (c) Mazzoni, R.; Salmi, M.; Zanotti, V. C-C Bond Formation in Diiron Complexes. Chem. Eur. J. 2012, 18, 10174-10194. (d) Knorr, M.; Jourdain, I. Activation of alkynes by diphosphine- and m-phosphido-spanned heterobimetallic complexes. Coord. Chem. Rev. 2017, 350, 217-247. (e) G. Li, D. Zhu, X. Wang, Z. Su, M. R. Bryce, Dinuclear metal complexes: multifunctional properties and applications. Chem. Soc. Rev., 2020, 49, 765-838.

14 H. W. Bosch, H.-U. Hund, D. Nietllspach, A. Salzer, General Route to the "Half-Open" Metallocenes C_5Me_5Ru(pentadienyl) and C_5Me_5Ru(diene)CI. X-ray Structures of an Optically Active Half-Open Metallocene and of a Dimetallic Ruthenabenzene Complex. Organometallics 1992, 11, 2087-2098.

15 W. Lin, S. R. Wilson, G. S. Girolami, Carbon-Carbon Bond Formation Promoted by Organoruthenium Complexes. The First Unsubstituted π-Metallabenzene Complex and Synthesis of the Tetramethyleneethane Complex. Organometallics 1997, 16, 2356-2361.

16 M. I. Bruce, N. N. Zaitseva, B. W. Skelton, A. H. White, Some reactions of allenylidene-ruthenium cluster carbonyls with alkynes. J. Chem. Soc., Dalton Trans. 2002, 1678-1686.

17 (a) F. Marchetti, Constructing Organometallic Architectures from Aminoalkylidyne Diiron Complexes. Eur. J. Inorg. Chem. 2018, 3987-4003, and references therein. (b) L. Biancalana, F. Marchetti,

Aminocarbyne ligands in organometallic chemistry. Coord. Chem. Rev. 2021, 449, 214203, and referencestherein. (c) G. Bresciani, S. Schoch, L. Biancalana, S. Zacchini, M. Bortoluzzi, G. Pampaloni and F. Marchetti, Cyanide – alkene competitionin a diiron complex and isolation of a multisite (cyano)alkylidene – alkene species. Dalton Trans., 2022, 51, 1936–1945. (d) G. Bresciani, L. Biancalana, G. Pampaloni, S. Zacchini, G. Ciancaleoni, F. Marchetti, A Comprehensive Analysis of the Metal–Nitrile Bonding in an Organo-Diiron System. Molecules 2021, 26, 7088.

18 G. Bresciani, S. Zacchini, G. Pampaloni, F. Marchetti, Carbon–Carbon Bond Coupling of Vinyl Molecules with an Allenyl Ligand at a Diruthenium Complex. Organometallics 2022, 41, 1006–1014.

19 (a) A. Boni, F. Marchetti, G. Pampaloni, S. Zacchini, Cationic Diiron and Diruthenium μ-Allenyl Complexes: Synthesis, X-Ray Structures and Cyclization Reactions with Ethyldiazoacetate/Amine Affording Unprecedented Butenolide- and Furaniminium-Substituted Bridging Carbene Ligands, Dalton Trans. 2010, 39, 10866-10875. (b) S. A. R. Knox, F. Marchetti, Additions and intramolecular migrations of nucleophiles in cationic diruthenium μ-allenyl complexes. J. Organomet. Chem. 2007, 692, 4119-4128.

20 S. A. R. Knox, F. Marchetti, Additions and intramolecular migrations of nucleophiles in cationic diruthenium μ-allenyl complexes. J. Organomet. Chem. 2007, 692, 4119-4128.

21 Luh, T.-Y. Trimethylamine N-Oxide-A Versatile Reagent For Organometallic Chemistry. Coord. Chem. Rev. 1984, 60, 255-276.

22 The crystallization procedure to collect X-ray quality crystals of complexes was complicated by their limited stability exhibited in organic solvents for prolonged time. For instance, **2** completely decomposed after one week in dichloromethane/diethyl ethe mixture at room temperature under N_2 atmosphere.

23 (a) H. Yang, C.-P. Chung, Y.-C. Lin, Y.-H. Liu, Facile oxygenation reactions of ruthenium acetylide complex containing substituted olefinic group, Dalton Trans. 2011, 40, 3703-3710. (b) K. A. Johnson, M. D. Vashon, B. Moasser, B. K. Warmka, W. L. Gladfelter, Significance of Carbenoid Character during the Protonation of Four- and Five-Membered Diruthenacycles Formed from the Reaction of $Ru_2(Me_2PCH_2PMe_2)_2(CO)_5$ with Dimethyl Acetylenedicarboxylate, Organometallics 1995, 14, 1, 461-470.

24 (a) M. A. Esteruelas, A.V.Gomez, A. M. Lopez, J. Modrego, E. Onate, Addition of Carbon Nucleophiles to the Allenylidene Ligand of $[Ru(\eta^5\text{-}C_5H_5)(CCCPh_2)(CO)(P^iPr_3)]BF_4$: Synthesis of New Organic Ligands by Formal C−C Coupling between Mutually Inert Fragments, Organometallics 1997,

16, 26, 5826-5835. (b) V. F. Kuznetsov, K. Abdur-Rashid, A. J. Lough, D. G. Gusev, Carbene vs Olefin Products of C-H Activation on Ruthenium via Competing α- and β-H Elimination, J. Am. Chem. Soc. 2006, 128, 44, 14388-14396.

25 (a) N. J. Forrow, S. A. R. Knox, M. J. Morris, A. G. Orpen, Synthesis, X-ray structure, and reactivity of $[Ru_3H_3(CO)_3(\eta\text{-}C_5H_5)_3]$: an entry into the organic chemistry of the triruthenium centre. J. Chem. Soc., Chem. Commun. 1983, 234-235. (b) P. J. King, S. A. R. Knox, G. J. McCormick, A. G. Orpen, Synthesis and reactivity of dimetallacyclopentenone complexes $[Ru_2(CO)(\mu\text{-}CO)\{\mu\text{-}C(O)CR1CR2\}(\eta\text{-}C_5H_5)_2]$ (R1 = Me or Ph; R2 = CO_2Me). J. Chem. Soc., Dalton Trans. 2000, 2975-2982. (c) C. Nataro, L. M. Thomas, R. J. Angelici, Cyclopentadienyl Ligand Effects on Enthalpies of Protonation of the Ru−Ru Bond in $Cp'_2Ru_2(CO)_4$ Complexes. Inorg. Chem. 1997, 36, 6000-6008. (d) C. Cesari, M. Bortoluzzi, C. Femoni, M. C. Iapalucci, S. Zacchini, One-pot atmospheric pressure synthesis of $[H_3Ru_4(CO)_{12}]^-$. Dalton Trans. 2021, 50, 9610-9622.

26 S. Noorizadeh, E. Shakerzadeh, Shannon entropy as a new measure of aromaticity, Shannon aromaticity, Phys. Chem. Chem. Phys. 2010, 12, 4742-4749.

27 (a) P. v. R. Schleyer, C. Maerker, A. Dransfeld, H. Jiao, N. J. R. v. E. Hommes, Nucleus-Independent Chemical Shifts: A Simple and Efficient Aromaticity Probe. J. Am. Chem. Soc. 1996, 118, 6317-6318. (b) Z. Chen, C. S. Wannere, C. Corminboeuf, R. Puchta, P. v. R. Schleyer, Nucleus-Independent Chemical Shifts (NICS) as an Aromaticity Criterion. Chem. Rev. 2005, 105, 3842-3888. (c) H. Fallah-Bagher-Shaidaei, C. S. Wannere, C. Corminboeuf, R. Puchta, P. v. R. Schleyer, Which NICS Aromaticity Index for Planar π Rings Is Best? Org. Lett. 2006, 8, 863-866.

28 S. Doherty, G. Hogarth, M. Waugh, W Clegg, M, R. J. Elsegood, Reactions of Alkynes with $[Fe_2(CO)_6(\mu\text{-}PPh_2)\{CH{=}C{=}CH_2\}]$: Formation of Diphenylvinylphosphine-Functionalized Vinyl Carbenes via Carbon-Carbon and Carbon-Phosphorus Bond Formation and Hydrogen Migration. Organometallics 2000, 19, 4557-4562.

29 (a) P. Blenkiron, S. M. Breckenridge, N. J. Taylor, A. J.; Carty, M. A. Pellinghelli, A. Tiripicchio, E. Sappa, Comparative chemistry of $\mu\text{-}\eta^1{:}\eta^2$-allenyl and $\mu\text{-}\eta^1{:}\eta^2$-acetylide complexes: η^5-cyclopentadienyl complexes via alkyne-allenyl coupling in the reactions of PhC≡CPh with $[Ru_2(CO)_6\{\mu\text{-}\eta^1{:}\eta^2\beta,\gamma\text{-}C(Ph){:}C{:}CH_2\}(\mu\text{-}PPh_2)]$ and $[Ru_2(CO)\{\mu\text{-}\eta^1{:}\eta^2\text{-}C{\equiv}CPh\}(\mu\text{-}PPh)]$. X-Ray structures of $[\{Ru(CO)\{\mu\text{-}\eta^2(C,O),\eta^5\text{-}CMePh\ (CH)(O)\}(\mu\text{-}PPh)\}_2]$ and $[Ru_2(CO)_5\{\mu\text{-}\eta^2(C,O),\eta^5\text{-}C_5HPh_2(C_6H_4)(O)\}(\mu\text{-}PPh_2)]$ J. Organomet. Chem. 1996, 506, 229-40. (b) S. M. Randall, N. J. Taylor, A. J. Carty, T. Ben Haddah, P. H. Dixneuf, Coupling of diphenylacetylene with $Ru_2(CO)_6$-$[\mu\text{-}\sigma, \eta^2\text{-}PhCC{=}CH_2](\mu\text{-}PPh_2)$, J. Chem. Soc. Chem. Commun. 1988, 13, 870-872.

30 R. D. Adams, S. Wang, The Coupling of Cumulenes to an Alkyne Ligand in an Osmium Cluster Complex The reactions of $Os_4(CO)_{11}(\mu_4\text{-}HC_2CO_2Me)(\mu_4\text{-}S)$ with allene and methyl isocyanate, Organometallics 1987, 6, 45-49.

31 T. Shibata, Y. Koga, K. Narasaka, Intra- and intermolecular allene-alkyne coupling reactions by the use of $Fe(CO)_4(NMe_3)$. Bull. Chem. Soc. Japan 1995, 68, 911-919.

32 H. Zhang, R. Lin, G. Hong, T. Wang, T. B. Wen, H. Xia, Nucleophilic Aromatic Addition Reactions of the Metallabenzenes and Metallapyridinium: Attacking Aromatic Metallacycles with Bis(diphenylphosphino)methane to Form Metallacyclohexadienes and Cyclic h^2-Allene-Coordinated Complexes. Chem. Eur. J. 2010, 16, 6999-7007.

33 F. Menges, "Spectragryph - optical spectroscopy software", Version 1.2.5, @ 2016-2017, http://www.effemm2.de/spectragryph.

34 G. R. Fulmer, A. J. M. Miller, N. H. Sherden, H. E. Gottlieb, A. Nudelman, B. M. Stoltz, J. E. Bercaw, K. I. Goldberg, NMR Chemical Shifts of Trace Impurities: Common Laboratory Solvents, Organics, and Gases in Deuterated Solvents Relevant to the Organometallic Chemist. Organometallics 2010, 29, 2176-2179.

35 W. Willker, D. Leibfritz, R. Kerssebaum, W. Bermel, Gradient selection in inverse heteronuclear correlation spectroscopy. Magn. Reson. Chem. 1993, 31, 287-292.

36 G. M. Sheldrick, Crystal structure refinement with SHELXL. Acta Crystallogr. C, 2015, 71, 3-8.

37 (a) Y. Minenkov, Å. Singstad, G. Occhipinti, V. R. Jensen, The accuracy of DFT-optimized geometries of functional transition metal compounds: a validation study of catalysts for olefin metathesis and other reactions in the homogeneous phase. Dalton Trans. 2012, 41, 5526-5541. (b) J.-D. Chai, M. Head-Gordon, Long-range corrected hybrid density functionals with damped atom-atom dispersion corrections. Phys. Chem. Chem. Phys. 2008, 10, 6615-6620. (c) I. C. Gerber, J. G. Ángyán, Hybrid functional with separated range. Chem. Phys. Lett. 2005, 415, 100-105.

38 F. Weigend, R. Ahlrichs, Balanced basis sets of split valence, triple zeta valence and quadruple zeta valence quality for H to Rn: Design and assessment of accuracy. Phys. Chem. Chem. Phys. 2005, 7, 3297–3305.

39 (a) M. Cossi, N. Rega, G. Scalmani, V. Barone, Energies, structures, and electronic properties of molecules in solution with the C-PCM solvation model. J. Comput. Chem. 2003, 24, 669–681. (b) V. Barone, M. Cossi, Quantum Calculation of Molecular Energies and Energy Gradients in Solution by a Conductor Solvent Model. J. Phys. Chem. A 1998, 102, 1995–2001.

40 (a) M. J. Frisch, G. W. Trucks, H. B. Schlegel, G. E. Scuseria, M. A. Robb, J. R. Cheeseman, G. Scalmani, V. Barone, B. Mennucci, G. A. Petersson, H. Nakatsuji, M. Caricato, X. Li, H. P. Hratchian, A. F. Izmaylov, J. Bloino, G. Zheng, J. L. Sonnenberg, M. Hada, M. Ehara, K. Toyota, R. Fukuda, J. Hasegawa, M. Ishida, T Nakajima, Y. Honda, O. Kitao, H. Nakai, T. Vreven, J. A. Montgomery Jr., J. E. Peralta, F. Ogliaro, M. Bearpark, J. J. Heyd, E. Brothers, K. N. Kudin, V. N. Staroverov, R. Kobayashi, J. Normand, K. Raghavachari, A. Rendell, J. C.Burant, S.S. Iyengar, J. Tomasi, M. Cossi, N. Rega, J. M. Millam, M. Klene, J. E. Knox, J. B. Cross, V. Bakken, C. Adamo, J. Jaramillo, R. Gomperts, R. E. Stratmann, O. Yazyev, A. J. Austin, R. Cammi, C. Pomelli, J. W. Ochterski, R. L. Martin, K. Morokuma, V. G. Zakrzewski, G. A. Voth, P. Salvador, J. J. Dannenberg, S. Dapprich, A. D. Daniels, Ö. Farkas, J. B. Foresman, J. V. Ortiz, J. Cioslowski, D. J. Fox, Gaussian 09, Revision C.01, Gaussian Inc., Wallingford, CT, 2010.

41 T. Lu, F. Chen, Multiwfn: A multifunctional wavefunction analyzer. J. Comput. Chem. 2012, 33, 580-592.